Non-nearest-neighbor dependence of the stability for RNA group II single-nucleotide bulge loops

MICHAEL D. MCCANN, GEOFFERY F.S. LIM, MICHELLE L. MANNI, JULIE ESTES, KELLY A. KLAPEC, GREGORY D. FRATTINI, ROBERT J. KNARR, JESSICA L. GRATTON, and MARTIN J. SERRA

Department of Chemistry, Allegheny College, Meadville, Pennsylvania 16335, USA

ABSTRACT

Thirty-one RNA duplexes containing single-nucleotide bulge loops were optically melted in 1 M NaCl, and the thermodynamic parameters ΔH°, ΔS°, ΔG°_{37}, and T_M for each sequence were determined. The bulge loops were of the group II variety, where the bulged nucleotide is identical to one of its nearest neighbors, leading to ambiguity as to the exact position of the bulge. The data were used to develop a model to predict the free energy of an RNA duplex containing a single-nucleotide bulge. The destabilization of the duplex by the bulge was primarily related to the stability of the stems adjacent to the bulge. Specifically, there was a direct correlation between the destabilization of the duplex and the stability of the less stable duplex stem. Since there is an ambiguity of the bulge position for group II bulges, several different stem combinations are possible. The destabilization of group II bulge loops is similar to the destabilization of group I bulge loops, if the second least stable stem is used to predict the influence of the group II bulge. In-line structure probing of the group II bulge loop embedded in a hairpin indicates that the bulged nucleotide is the one positioned farther from the hairpin loop.

Keywords: bulge loops; RNA secondary structure; thermal stability; in-line probing

INTRODUCTION

RNA is central to life processes. Among these are the control of gene expression (Chung et al. 2006), intron splicing (Schmelzer and Schweyen 1986; Suzuki et al. 2006), protein synthesis and catalysis (Doudna et al. 1989; Krasovska et al. 2006), ligand binding (Harper and Logsdon 1991), and virus replication (Roy et al. 1990). Recent discoveries have highlighted the regulation of gene expression by microRNAs (miRNAs) (Matzke and Birchler 2005) and riboswitches (Tinsley et al. 2007). Given its versatility in a wide variety of biological functions, RNA has been recognized as much more than a passive intermediary between DNA and proteins.

The functional diversity of RNA is achieved by the hierarchical folding of RNA into complex three-dimensional (3D) structures (Brion and Westhof 1997; Tinoco and Bustamante 1999). To understand the mechanism of action of RNA at the atomic level, the structure of RNA must be known. Since secondary structure generally forms faster and is significantly more stable than the tertiary structural elements, secondary structure can often provide clues to the 3D folding of the RNA. For this reason, there is interest in predicting the secondary structure of RNA from sequence. The most common programs for secondary structure prediction (Mfold [Zuker 2003], RNAstructure [Mathews et al. 2004], and the Vienna package [Hofacker et al. 1994]) use thermodynamic values to predict the most stable secondary structures.

Current structure prediction methods predict ~73% of the known base pairs for an RNA sequence. Improvement in the thermodynamic parameters for the secondary structural motifs should result in improvements in the accuracy of secondary structural prediction.

Bulges are regions of unpaired nucleotides situated along one strand of a nucleic acid duplex. The most common bulge found in nature consists of a single nucleotide, although sizes can vary up to hundreds of nucleotides in length. Single-nucleotide bulge loops are classified into four distinct groups (Blose et al. 2007). Group I bulge loops are those in which the bulged nucleotide is not identical to either of its nearest-neighbor nucleotides. Group II bulge loops, on the other hand, are identical to at least one nearest neighbor (Table 1). Whereas the bulged nucleotide of the group I category can be known with confidence, the positions of group II bulges are ambiguous since nearest neighbors can form base pairs with the

Reprint requests to: Martin J. Serra, Department of Chemistry, Allegheny College, 520 North Main Street, Meadville, PA 16335, USA; e-mail: mserra@allegheny.edu; fax: (814) 332-2789.

Article published online ahead of print. Article and publication date are at http://www.rnajournal.org/cgi/doi/10.1261/rna.2306911.

TABLE 1. Example of group II bulge loop ambiguity

Sequence	Potential bulge positions	
CGCCGCC GCG CGG	CGCCGCC GCG CGG	CGCCGCC GC GCGG
Duplex sequence (-ΔG°_{37} kcal/mol)	CGCGCC (10.7) GCGCGG	CGCGCC (10.7) GCGCGG
Stem to left of bulge (-ΔG°_{37} kcal/mol)	CGC GCG (5.8)	CG GC (2.4)
Stem to right of bulge (-ΔG°_{37} kcal/mol)	GCC CGG (6.7)	CGCC GCGG (9.0)

bulged nucleotide. Group III bulges have ambiguity in both the position and identity of the bulged nucleotide, and group IV bulge loops combine facets of both group II and group III bulge loops.

Recent investigations have revealed significant roles of bulge loops in biological processes. Bulges can be exploited for specific recognition by various proteins (Lilley 1995). Multiple factors of a bulge loop, including size, sequence identity, and location within the RNA architecture, are attributed to its function in vivo. For instance, the splicing efficiency of target sites in oligonucleotide-based artificial nuclease systems was found to be dependent on bulge size (Åström et al. 2003). Sequence variants of a double-nucleotide bulge in domain 5 of the yeast mitochondrial intron alγ showed reduced rates of self-splicing, highlighting the role of this secondary motif as an intron–exon splice site (Schmidt et al. 1996). Individual bulge loops often perform more than one function, as in the case of a six-nucleotide bulge in the RNA intermediate of the hepatitis B virus. Specific packaging of the transcript into viral capsids is mediated by the interaction of reverse transcriptase with the 5′-proximal part of the bulge in the RNA. While the 5′-proximal part of the bulge is involved in protein binding, the 3′-distal end has a special role as the template for the first nucleotides of (−)strand DNA during reverse transcription (Rieger and Nassal 1995).

In this study, the complete set of group II single-nucleotide bulge loops with Watson-Crick nearest neighbors has been thermodynamically characterized to improve our ability to predict the stability of RNA duplexes with bulge loops. As with the group I bulge loops (Blose et al. 2007), the free-energy increment for the insertion of a bulge into an RNA duplex was primarily influenced by non-nearest-neighbor interactions. In particular, the stability of the stems adjacent to the bulged nucleotide influences the impact of the bulged nucleotide on the stability of the duplex. In addition, the position of the ambiguous group II bulge loops was determined using in-line probing.

MATERIALS AND METHODS

RNA synthesis and purification

Most oligomers were synthesized on CPG solid supports (Applied Biosystems 392 DNA/RNA Synthesizer) utilizing phosphoramidites with the 2′-hydroxyl protected as the *tert*-butyl dimethylsilyl ether from Glen Research (Usman et al. 1987; Wincott et al. 1995). Oligomers underwent ammonia and fluoride deprotection, and a crude sample was purified using preparative *tlc* (*n*-propanol:ammonium hydroxide:water, 55:35:10) and Sep-Pak C18 (Waters) chromatography. Some oligomers were ordered from Dharmacon, and deprotection of the oligomers was carried out using the manufacturer's instructions. The oligomers were then purified as described above. Sample purity was determined through analytical *tlc* or HPLC (PRP-1; Hamilton) and was >95%.

Melting curve and data analysis

For non-self-complementary sequences, individual strand concentrations were calculated from high-temperature single-strand absorbance at 260 and 280 nm using nearest-neighbor extinction coefficients (Borer 1975; Richards 1975). Single strands were then annealed in a 1:1 molar ratio. Optical melting experiments were performed using a Beckman DU 640 Spectrophotometer and High Performance Temperature Controller at 260 or 280 nm. Absorbance changes for oligomers in 1 M NaCl melt buffer (1 M NaCl, 0.01 M cacodylic acid, 0.001 M EDTA at pH 7.0) were recorded as a function of temperature from 95°C to 10°C at a rate of 1°C/min as described previously (Serra et al. 1994). The experiment was repeated at 10 varying sample concentrations to give at least a 50-fold concentration range (10 μM–1 mM) for each sample. Absorbance-versus-temperature profiles were fit to a two-state model with sloping base lines using a nonlinear least squares program (McDowell and Turner 1996). Thermodynamic parameters for duplex formation were obtained by two methods: (1) enthalpy and entropy changes from the fits of the individual melting curves were averaged; and (2) plots of the reciprocal melting temperature, T_M^{-1}, versus $\log(C_t/4)$ gave enthalpy and entropy changes (Borer et al. 1974):

$$T_M^{-1} = (2.3\ R/\Delta H^{\circ}) \log(C_t/4) + (\Delta S^{\circ}/\Delta H^{\circ}) \qquad (1)$$

Here, C_t is the total concentration of oligomer. Parameters derived from the two methods generally agreed within 15%, consistent with the two-state model (Freier et al. 1986; Allawi and SantaLucia 1997). The Gibbs free energy change at 37°C was calculated as:

$$\Delta G^{\circ}_{37} = \Delta H^{\circ} - (310.15\text{K})\,\Delta S^{\circ} \qquad (2)$$

Determination of the contribution of bulge loops to duplex thermodynamics

The free energy of duplex formation can be approximated by the nearest-neighbor model (Xia et al. 1998). The free energy contribution of each bulged nucleotide was calculated from the experimental data and the nearest-neighbor model according to Equation 3, where $\Delta G^\circ_{37(\text{measured})}$ is the experimentally determined value from the melts and

$$\Delta G^\circ_{37(\text{bulge})} = \Delta G^\circ_{37(\text{measured})} - \Delta G^\circ_{37(\text{duplex})} \quad (3)$$

$\Delta G^\circ_{37(\text{duplex})}$ is calculated from the nearest-neighbor model for the duplex as if it did not contain the bulge. ΔH° values are calculated in a similar fashion.

Phylogenetic analysis

A database of phylogenetically determined RNA secondary structures (Cannone et al. 2002) of 305 SSU rRNAs, 169 LSU rRNAs, 16 group I RNAs, and seven group II RNAs was compiled. The database was searched for group II single-nucleotide bulge loops. A total of 768 group II bulge loops was identified. The loops were characterized by nearest-neighbor base pairs and bulge identity.

In-line probing

Samples for in-line probing were labeled at either the 5′ or 3′ end during synthesis with fluorescein (Glen Research) or purchased from IDT. The RNAs were purified as described above except that non-fluorescent *tlc* plates were used and the RNA was detected by the fluorescent label. The RNA was incubated in 50 mM Tris (pH 8.3), 20 mM $MgCl_2$, and 100 mM KCl for 1–2 d at room temperature in the dark (Soukup and Breaker 1999; Regulski and Breaker 2008). The cleavage products were analyzed by chromatography on non-fluorescent *tlc* plates (*n*-propanol:ammonium hydroxide:water; the percentage of *n*-propanol was varied between 65% and 80% to maximize separation of the cleavage products, and water was maintained at 10%). The fluorescent products were analyzed with a Kodak Image Station 400MM Pro.

Statistical analysis

Statistical analysis of the data was done using the statistical software available with GraphPad Prism and GraphPad Instat.

RESULTS

For a limited number of group II sequences (five), we have previously shown that insertion of a group II bulge into an RNA duplex was less destabilizing than the insertion of a group I bulge (Znosko et al. 2002). To determine the impact of the bulge identity and the nearest neighbors on the stability of group II bulge loops, 31 additional (16 purine and 15 pyrimidine bulges) duplexes containing a group II single-nucleotide bulge loop were prepared, and the thermodynamics of duplex formation was measured by optical melting. These oligomers, when combined with the previously measured oligomers, give measurements for the complete set of group II single-nucleotide bulge loops with Watson-Crick nearest neighbors.

Thermodynamic parameters for duplex formation by these oligonucleotides are listed in Table 2. The oligonucleotides are listed in order of decreasing free energy for the respective duplex. Sequences were divided into two groups: duplexes with purine bulges; and duplexes with pyrimidine bulges. Residues in bold are the bulge nucleotides. The parameters are the average values derived from fits of the melt curves and from T_M^{-1} versus $\log(C_t/4)$ plots. Data from both methods agree within 15% for all duplexes in Table 2, consistent with the two-state model with the exception of

$$\begin{pmatrix} 5'GCAGUUGAG \\ 3'CGUCA\ CUC \end{pmatrix}$$

and

$$\begin{pmatrix} 5'GCAGAAGAGCG \\ 3'CGUCU\ CUCGC \end{pmatrix}$$

(Freier et al. 1986; Allawi and SantaLucia 1997). The average deviations in thermodynamic parameter values are 8.3%, 9.5%, and 1.7% for ΔH°, ΔS°, ΔG°_{37}, respectively.

The free energy contribution of each bulged nucleotide was calculated from the experimental data according to Equation 3 and is presented in Table 3. As previously observed (Longfellow et al. 1990; Znosko et al. 2002; Blose et al. 2007), all of the bulges destabilize the duplex. The extent of destabilization ranges between 0.9 and 7.3 kcal/mol. The destabilization caused by the introduction of a single group II pyrimidine bulge into a duplex is 3.7 ± 1.3 kcal/mol and for a purine residue is 4.0 ± 0.9 kcal/mol. Since these values are not statistically different, they can be combined to provide a simple model to predict the stability of a duplex containing a single group II bulge nucleotide (purine or pyrimidine), which is just the average of all the measured values: 3.8 kcal/mol. Unlike our initial analysis that showed that group II bulge loops had a smaller influence on duplex formation (Znosko et al. 2002), the additional measurements show that the influence of a group II single-nucleotide bulge loop is similar to the influence of group I single-nucleotide bulge loops.

The enthalpic contribution for single-nucleotide group II bulge loops are also presented in Table 3. In all cases, except

TABLE 2. Thermodynamic parameters for duplex formation for oligonucleotides containing a group II bulge

	T_M^{-1} vs. log C_T plots				Average of curve fits			
Oligomers[a]	$-\Delta H°$ (kcal/mol)	$-\Delta S°$ (eu)	$\Delta G°_{37}$ (kcal/mol)	T_M (°C)[b]	$-\Delta H°$ (kcal/mol)	$-\Delta S°$ (eu)	$-\Delta G°_{37}$ (kcal/mol)	T_M (°C)[b]
Group II purine								
CUGGCC**GG**UC GACCGG CAG	81.6	214.6	15.0	72.9	71.6	185.4	14.1	73.7
GCAG**AA**GAGCG CGUCU CUCGC	98.0	270.5	14.1	62.9	83.2	226.1	13.1	63.5
AGCU**GG**CAG UCGAC GUC	57.2	153.6	9.6	54.6	56.0	149.5	9.6	55.1
GACC**AA**UAGC CUGGU AUCG	76.0	213.3	9.9	51.2	75.0	209.8	9.9	51.7
GAGU**AA**GAGC CUCAU CUCG	84.6	240.8	9.9	49.9	90.0	257.9	10.0	49.6
GACG**AA**UAGC CUGCU AUCG	68.4	191.0	9.2	49.4	68.4	190.8	9.2	48.8
CUGC**GG**UCG GACGC AGC	62.0	171.6	8.7	48.4	69.7	196.0	8.9	48.0
CGAC**GG**CAG GCUGC GUC	69.4	195.2	8.8	47.6	68.6	192.8	8.8	47.7
CAC**AA**GCAC GUGU CGUG	56.8	156.8	8.2	46.2	58.9	163.6	8.2	46.0
GCUU**AA**CCUG CGAAU GGAC	73.2	208.3	8.6	45.9	68.3	193.2	8.4	45.6
GCAG**AA**CAG CGUCU GUC	48.9	133.7	7.4	42.8	52.7	145.2	7.7	44.0
GACU**AA**UGAC CUGAU ACUG	56.3	156.7	7.7	43.5	56.0	156.2	7.5	42.5
CAU**GG**UGC GUAC ACG	38.4	103.0	6.4	35.9	42.2	115.2	6.4	36.1
GAC**AA**CCUG CUGU GGAC	37.9	102.9	6.0	32.3	38.6	105.0	6.0	32.9
Group II pyrimidine								
CGGG**CC**ACG GCCCG UGC	72.7	195.6	12.0	62.3	65.7	174.3	11.6	63.0
GAG**CC**GGUC CUCG CCAG	48.5	124.3	9.9	60.2	47.2	120.2	10.0	61.2
GAU**CC**GGUC CUAG CCAG	50.0	132.9	8.8	51.7	54.4	146.6	9.0	51.5
GCCG**UU**GC CGGCA CG	61.1	167.7	9.1	50.5	55.8	151.1	8.9	51.0
GCUG**CC**UCUG CGACG AGAC	48.1	128.3	8.3	48.8	41.9	108.2	8.3	50.9

(*continued*)

TABLE 2. *Continued*

	T_M^{-1} vs. log C_T plots				Average of curve fits			
Oligomers[a]	$-\Delta H°$ (kcal/mol)	$-\Delta S°$ (eu)	$\Delta G°_{37}$ (kcal/mol)	T_M (°C)[b]	$-\Delta H°$ (kcal/mol)	$-\Delta S°$ (eu)	$-\Delta G°_{37}$ (kcal/mol)	T_M (°C)[b]
CGUGU**CC**G GCACAG C	51.1	137.1	8.6	50.0	57.8	157.9	8.8	49.8
CUG**CC**GUCG GACG CAGC	64.1	178.6	8.8	48.2	68.7	192.5	9.0	48.4
GCAG**UU**GAG CGUC ACUC	54.6	148.6	8.4	48.5	72.8	206.2	8.8	47.0
CAGG**UU**AGC GUCCA UCG	55.7	152.9	8.3	47.2	62.5	174.3	8.4	46.7
CGA**CC**GCAG GCUG CGUC	55.1	152.5	7.8	44.5	53.9	148.8	7.8	44.4
GAGA**UU**GUC CUCUA CAG	56.4	158.4	7.3	41.2	59.6	168.3	7.4	41.2
CACA**UU**ACAC GUGUA UGUG	101.7	304.2	7.4	39.5	89.6	265.3	7.3	39.7
GGU**CC**UUCG CCAG AAGC	63.6	185.5	6.7	37.8	56.3	159.9	6.7	38.0
GCAA**CC**UAC CGUUG AUG	43.4	117.9	6.8	39.2	51.4	144.4	6.7	37.7
GCUU**CC**UG CGAAG AC	52.0	148.9	5.9	33.0	55.6	160.5	5.8	33.1

Solutions are 1.0 M NaCl, 10 mM sodium cacodylate, 0.5 mM EDTA (pH 7).
[a]Nucleotides in bold are the potential bulge residue. Top sequence is written 5′ → 3′.
[b]Calculated at 10^{-4} M oligomer concentration.

two, the introduction of a bulge decreases the enthalpy of formation of the duplex. As with the free energy, the enthalpy contribution to duplex formation is nearly identical for pyrimidine and purine bulge nucleotides. Therefore, the enthalpy contribution for group I single-nucleotide bulge loops is just the average of the measured values (13.4 ± 9.4 kcal/mol). As noted previously, the standard error for enthalpy measurements is much larger than for free energy measurements (Lu et al. 2006). The enthalpy for the group II bulges is slightly larger than the enthalpy for group I bulges (14.1 ± 9.2 kcal/mol) (Blose et al. 2007). The enthalpy values presented in Table 3 can be used in conjunction with the free energy and enthalpy parameters for other nearest-neighbor motifs to determine the stability of RNA structures at temperatures other than 37°C (Lu et al. 2006); however, the range of enthalpic values makes this extrapolation problematic.

Twelve additional group II bulge loops were investigated where the bulge was adjacent to two identical nucleotides such that there are three possible bulged nucleotides. The thermodynamics for duplex formation by these oligomers are presented in Table 4. Data from both fitting methods agree within 15% for all duplexes in Table 3, consistent with the two-state model. The average deviations in thermodynamic parameter values are 9.6%, 10.9%, and 1.7% for $\Delta H°$, $\Delta S°$, and $\Delta G°_{37}$, respectively.

In-line probing takes advantage of the natural instability of RNA to detect single-stranded regions in RNA. The structural flexibility of single-stranded regions allows the RNA to examine additional structural conformations, some of which produce an in-line arrangement of the 2′-alcohol and the 5′-O of the phosphodiester, leading to a favorable transition state and cleavage of the RNA strand at the site of flexibility. In-line probing was used to resolve the ambiguity as to the identity of the group II bulged nucleotide. Because of the small size of our RNA oligomers, we used analytical *tlc* to resolve the products of in-line cleavage. The hairpin motif was chosen because at the low concentrations of RNA used in the in-line probing experiments, a duplex would be primarily single-stranded. Figure 1A displays the chromatogram of the treated and untreated RNA. Initially, we investigated the

TABLE 3. Thermodynamic parameters and natural occurrence for group II bulges

Bulge sequence[a]	$\Delta G°_{37(bulge)}$ (kcal/mol)[b]	$\Delta H°_{bulge}$ (kcal/mol)[b]	Percentage of naturally occurring group I sequences[c]	Bulge sequence[a]	$\Delta G°_{37(bulge)}$ (kcal/mol)[b]	$\Delta H°_{bulge}$ (kcal/mol)[b]	Percentage of naturally occurring group I sequences[c]
CAAC	6.3	38.2		ACCA	2.4[d]	12.2[d]	
GU G			7.0	UG U			3.3
CAAG	4.0, 3.2[d]	18.1,13.2[d]		ACCG	5.0	22.8	
GU C	1.7, 1.7	13.2, 10.8	32.4	UG C			1.2
CAAU	3.9	11.0		ACCU	3.5	22.1	
GU A			6.1	UG A			0.1
GAAC	4.7	26.1		GCCA	3.1	12.0	
CU G			4.0	CG U			6.0
GAAG	3.7[d]	13.0[d]		GCCG	3.9	10.9	
CU C	4.6	12.9	5.5	CG C	4.0	34.2	1.3
GAAU	3.9	17.3		GCCU	7.3	45.9	
CU A			1.8	CG A			1.3
UAAC	4.9	11.2		UCCA	2.3[d]	14.3[d]	
AU G			3.6	AG U			0.1
UAAG	3.8	−0.6		UCCG	3.0	26.3	
AU C			4.6	AG C	0.9	8.9	0.4
UAAU	4.1	25.9		UCCU	4.8	14.0	
AU A			4.9	AG A	3.0	8.1	4.9
CGGC	4.0[d]	9.5[d]		AUUA	4.0	−16.7	
GC G	4.0	8.3	0.5	UA U			3.4
CGGU	4.0	11.4		AUUG	3.1	17.4	
GC A	2.4	16.9	1.0	UA C			0.9
UGGC	3.2	18.2		GUUA	4.0	16.1	
AC G			1.4	CA U			1.7
UGGU	2.6	23.1		GUUG	3.7	13.5	
AC A			0.7	CA C	3.7	13.3	1.7

[a]The top strand is written 5′ → 3′.
[b]Values were calculated as described in text.
[c]The total number of single-nucleotide group II bulge loop sequences closed by Watson-Crick base pairs found in the database described in Material and Methods is 768.
[d]From Znosko et al. (2002).

in-line probing of a fully base-paired hairpin. The only products detected were fluorescein end label and a monomer, probably generated by breathing of the terminal base pair (Fig. 1A, lane 3). No cleavage was observed within the hairpin loop which while single-stranded is a highly structured tetraloop. As expected, the control lane (Fig. 1A, lane 4) displays only a full-length hairpin. We then examined a group I bulge loop embedded into the stem of a hairpin loop. In addition to the cleavage of the fluorescein end label and monomer, cleavage at the 3′ side of the bulged loop position (tetramer) was observed as expected. Again, the untreated hairpin shows almost exclusively full-length material. We investigated a hairpin with a stem containing a group II bulge loop. As observed with the group I hairpin, we initially observed cleavage at the fluorescein end label and monomer. The major product (90%) from the cleavage of the group II bulge loop co-migrates with the tetramer in the chromatogram (Fig. 1B), indicative of cleavage at the "blue" 5′ adenosine residue. The remaining cleavage product (10%) co-migrates as a pentamer, indicative of minor cleavage at the "red" 3′ adenosine.

We then used in-line probing to determine the identity of the bulged nucleotide for three additional sets of group I and group II hairpins. For the group I hairpins, cleavage was always observed to the 3′ side of the bulged nucleotide, irrespective of whether the bulge was located to the 5′ or 3′ side of the hairpin loop (data not shown). For the group II hairpins, cleavage occurred in all examples exclusively or primarily at the residue that would place the bulged nucleotide further from the hairpin loop. These results are summarized in Table 5.

DISCUSSION

We previously examined the sequence dependence of stability for the complete set of group I single-nucleotide bulge loops. The results led to a model to improve our ability to predict the stability of RNA duplexes with bulge loops. Non-nearest-neighbor interactions were shown to play a significant role in bulged nucleotide stability. Specifically, as the stability of the less stable stem of the duplex decreases, the destabilization of the duplex caused by the bulge loop decreases (Blose et al. 2007).

TABLE 4. Thermodynamic parameters for duplex formation for oligonucleotides containing a group II bulge with three identical contiguous bases

	T_M^{-1} vs. log C_T plots				Average of curve fits			
Oligomers[a]	$-\Delta H°$ (kcal/mol)	$-\Delta S°$ (eu)	$\Delta G°_{37}$ (kcal/mol)	T_M (°C)[b]	$\Delta H°$ (kcal/mol)	$-\Delta S°$ (eu)	$-\Delta G°_{37}$ (kcal/mol)	T_M (°C)[b]
Group II purine								
GUC**GGG**CC CAGC CGG	54.0	141.3	10.1	59.2	53.6	139.9	10.2	59.7
GCU**GGG**CUG CGAC CGAC	59.8	161.1	9.9	55.3	59.4	159.9	9.8	55.2
CAGG**AAA**GC GUCCU UCG	53.0	147.6	7.2	40.9	52.5	145.7	7.3	41.7
GAC**AAA**GUC CUGU UCAG	61.7	176.8	6.9	38.8	61.0	174.2	6.9	39.1
Group II pyrimidine								
CGG**CCC**ACG GCCG GUGC	71.2	192.8	12.1	63.1	78.2	211.6	12.6	63.1
GCU**CCC**UAC CGAG GAUG	56.7	152.7	9.3	53.2	62.2	169.6	9.6	52.9
GA**CCCC**AG CUGG GUC	50.0	132.6	8.9	52.3	52.9	141.4	9.0	52.4
CGA**CCC**UCC GCUG GAGG	70.6	193.5	10.6	55.9	71.0	197.7	9.8	51.7
UGA**CCC**UCA ACUG GAGU	67.3	186.9	9.3	50.5	68.2	189.7	9.4	50.6
GCA**CCC**AUG CGUG GUAC	55.8	151.7	8.7	49.8	53.4	144.2	8.7	50.2
GCG**UUU**GAG CGCA ACUC	63.1	177.4	8.1	44.7	62.9	176.7	8.1	44.9
GCA**CCC**GUG CGUG GCAC	60.4	169.2	7.9	44.4	71.6	204.6	8.1	44.1

Solutions are 1.0 M NaCl, 10 mM sodium cacodylate, 0.5 mM EDTA (pH 7).
[a]Nucleotides in bold are the potential bulge residue. Top sequence is written 5′ → 3′.
[b]Calculated at 10^{-4} M oligomer concentration.

Nearest-neighbor influences on the thermodynamics of group II bulge loops

In an earlier investigation using a limited number of group II bulge loops (Znosko et al. 2002), we suggested that group II bulge loops were less destabilizing than group I bulge loops when inserted into an RNA duplex. The range of free energy contributions of the group II bulge loops to duplex formation listed in Table 3 is large (0.9–7.3 kcal/mol). To investigate the influence of the bulge nearest neighbor on the thermodynamic contribution of the bulge on duplex formation, we examined the thermodynamic contribution of the bulge loops versus the free energy of the nearest neighbors. Note that because of the ambiguity in the position of the group II bulge loops (Table 1), two possible nearest-neighbor interactions are possible. For this analysis, we used the average of the two values as the free energy of the nearest neighbor. Since (for the group I bulge loops) the free energy contribution of the bulge did not depend on the identity of the bulge, we included all of the bulge loop values from Table 3 as a single data set. Figure 2 displays the plot for this analysis. The first conclusion to be drawn from the results is that since the slope of the regression line is not significantly different from zero (-0.032 ± 0.42), the identity of the bulge loop nearest neighbors does not influence the thermodynamics for group II bulge loop

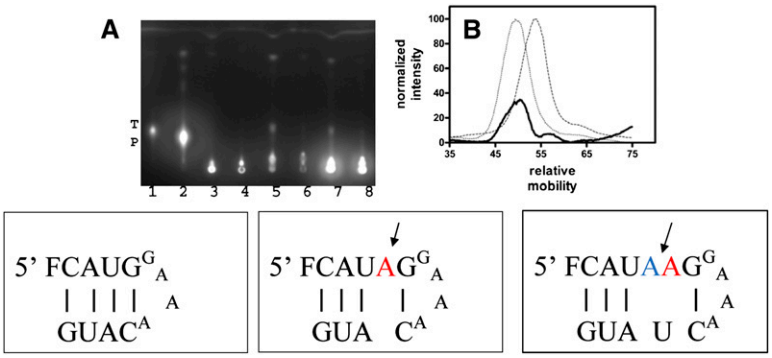

FIGURE 1. (*A*) *tlc* analysis of in-line probing of group I and group II bulge loops. (Lane *1*) T, tetramer, 5′-end-labeled with fluorescein. (Lane *2*) P, pentamer, 5′-end-labeled with fluorescein. (Lane *3*) Cleavage of fully base-paired hairpin; sequence given in figure. (Lane *4*) Control lane for fully base-paired hairpin. (Lane *5*) Cleavage for group I hairpin; sequence given in figure. (Lane *6*) Control lane for group I cleavage. (Lane *7*) Cleavage of group II hairpin; sequence given in figure. (Lane *8*) Control lane for the group II cleavage. (*B*) Histogram of the fluorescent intensity for the group II in-line cleavage, size standards: (. . .) tetramer; (- - -) pentamer. Hairpin figures indicate position of bulge and cleavage site.

insertion on duplex formation. Second, the thermodynamic influence of group II bulge loops on duplex formation (average value 3.8 kcal/mol) is very similar to that observed previously for group I bulge loops (4.0 kcal/mol) (Blose et al. 2007).

That the free energy increment for the insertion of a bulge loop into an RNA duplex is independent of both the identity of the bulge and its nearest neighbors is in marked contrast to the influence of bulge loops in a DNA helix, where both the bulge identity and nearest neighbors were shown to influence the stability of the insertion of a bulge (Tanaka et al. 2004; Conceicao et al. 2010). Also in contrast to our results where the insertion of a bulge always leads to destabilization of the duplex, the insertion of a bulge into a DNA duplex can result in helix stabilization. It is not clear why bulge loops would result in different influences on RNA and DNA duplexes. Using temperature gradient gel electrophoresis, Wartell (Zhu and Wartell 1999) has shown that group II bulge loops in DNA and RNA were more stable than group I bulge loops, although the effect was small (0.3 kcal/mol). We may not see this small effect because of the larger influence of non-nearest-neighbor interactions on bulge loop stability (see below).

Non-nearest-neighbor influences on the thermodynamics for group II bulge loops on duplex formation

The main determinant of the thermodynamic influence of group I bulge loops on duplex formation was shown to be due to non-nearest-neighbor influences. Specifically, the stability of the stem affects the extent to which insertion of the bulge loop destabilized the duplex. To determine if group II bulge loops are also influenced by the stability of the stems adjacent to the bulge, we examined how the stability of the adjacent stem influences the thermodynamics of group II bulge loop insertion into a duplex. The conformational ambiguity of the group II bulge loop allows for two possible sets of stems (Table 1) and, therefore, four possible stems. We first examined the influence of the bulge versus the stability of the least stable stem. These results are presented in Figure 3A. For a given stability of stem, it appears that the group II bulge loops destabilize the duplex more than a group I bulge loop. We then examined the influence of the bulge versus the stability of the second least stable stem. These results are presented in Figure 3B. Now, for a given stability of a stem, it appears that the group II bulge loops destabilize the duplex to the same extent as a group I bulge loop. In fact, the linear fit of the data give the following:

$$\Delta G^{\circ}_{37(\text{group I bulge loop})} = -0.62\ \Delta G^{\circ}_{\text{less stable stem}} + 0.25$$

for the group I and

$$\Delta G^{\circ}_{37(\text{group II bulge loop})} = -0.54\ \Delta G^{\circ}_{\text{second least stable stem}} + 0.46$$

for group II bulges.

The linear fits for influence of the group I and group II bulges are nearly identical.

Enthalpic contributions of group II single-nucleotide bulge loops on duplex formation

Since the free energy increment for the insertion of a bulge loop was dependent on the stability of the stem adjacent to the bulge, we investigated the influence of stem stability on the enthalpy of bulge insertion. Figure 4 displays the

TABLE 5. Summary of in-line cleavage results

	Percentage cut at red (3') bulged adenosine	Percentage cut at blue (5') bulged adenosine
5' CA U GU G A || || A FGUAACA A	>95	
5' CUA U G G A ||| | A FGAUAAC A	80	20
5' FCAUAAG G A ||| | A GUA U C A	10	90
5' FCAAGAU G A | ||| A G U CUA A		>95

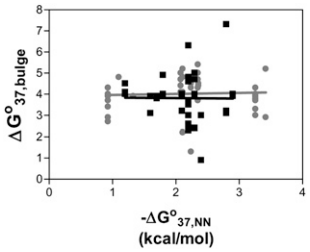

FIGURE 2. Plot of free energy change for bulge loop formation, $\Delta G^\circ_{37(\text{bulge})}$, versus the free energy increment, $\Delta G^\circ_{37(\text{nn})}$, for the nearest-neighbor interaction at the site of the group II bulge loops (black box) and group I bulge loops (gray circle) (Blose et al. 2007). (Dark solid line) The linear regression line for the group II data; (light solid line) the linear regression line for the group I data.

enthalpy of bulge insertion as a function of the stability of the second least stable stem for group II bulge loops. As previously observed for the group I bulges, the least-squares fit of data did not have a slope significantly different from zero, suggesting that the average enthalpy value (13.4 ± 9.4 kcal/mol) is a reasonable approximation for the enthalpic energy contribution. The enthalpic contribution due to a group II bulge loop is not statistically different from the value obtained for the group I bulge loops (16.0 ± 10.7 kcal/mol); all of the enthalpic values for group I and group II bulge loops can be combined for an average value of 14.7 ± 9.9 kcal/mol. The enthalpic values can be used in conjunction with the free energy parameters to determine the stability of RNA structures at temperatures other than 37°C.

Phylogenetic analysis of group II single-nucleotide bulge loop

The database examined in this study contained 768 group II single-nucleotide bulge loops. Group II bulge loops are less numerous than the group I bulge loops (3520 closed by Watson-Crick base pairs). The frequencies of occurrence of the group II single-nucleotide bulge loops are listed in Table 3. As observed with the group I bulge loops, nearly 70% of the total represent adenosine bulges. No other sequence occurs more frequently than 4% except (G**CC**A/CG U) or (U**CC**U/AG A). Since the stability of group II single-nucleotide bulge loops is independent of the identity of the bulge, there is no correlation between the thermodynamic contribution of the bulge and its frequency of occurrence. Therefore, the selection of naturally occurring bulge nucleotides must be related to factors other than stability.

Thermodynamic contribution from group II bulge loop with more than two identical nearest neighbors

We examined the thermodynamic stability of 12 additional duplexes that contained a bulge loop, but with two identical nearest neighbors, so that there were three possible positions for the bulged nucleotide (Table 4). We examined the influence of the adjacent stem stability on the thermodynamic contribution of these group II bulge loops on duplex formation (Fig. 5). The thermodynamic contribution of the group II bulge loops with three possible bulge positions, using the second least stable stem, leads to a relationship that is nearly identical ($\Delta G^\circ_{37(\text{group II bulge loop})} = -0.52\,\Delta G^\circ_{\text{second least stable stem}} + 1.0$) to that for the group II bulge loops with only two possible bulge positions. Therefore, the model derived earlier can be used to predict the thermodynamic contribution of all group II bulge loops irrespective of the number (two or three) of identical nearest neighbors. Combining all of the data from group I and group II bulge loops can then be used to derive a single relationship to predict the thermodynamic contribution of bulge loops:

$$\Delta G^\circ_{37(\text{group I bulge loop})} = -0.53\ \Delta G^\circ_{\text{stem}} + 0.7 \qquad (4)$$

where $\Delta G^\circ_{\text{steam}}$ is the less stable stem for group I bulge loops and the second least stable stem for group II bulge loops.

We then used Equation 4 to predict the $\Delta G^\circ_{37\ \text{bulge loop}}$ for all of the bulge loops in Table 3. The results are presented in the Supplemental Material. The average difference between the measured and predicted values was 0.7 kcal/mol. This is reasonably good given the wide range in $\Delta G^\circ_{37\ \text{bulge loop}}$ values (7.3–0.9 kcal/mol). For example, if we consider the four measured values for the most prevalent group II bulge loop CAAG/GU C: 4.0, 3.2, 1.7, and 1.7 kcal/mol; using Equation 4, the predicted values for these four group II bulge loops based on the duplex into which they are embedded are

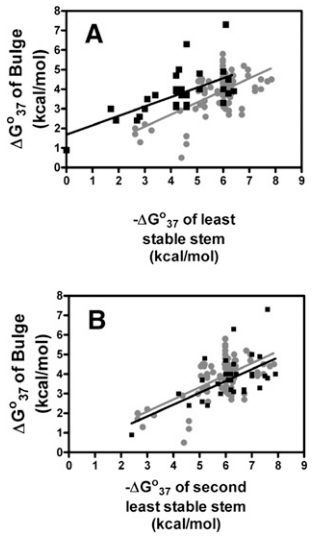

FIGURE 3. (*A*) Plot of free energy change for group II bulge loop formation, $\Delta G^\circ_{37(\text{bulge})}$, versus free energy of the least stable duplex stem. (*B*) Plot of free energy change for bulge loop formation, $\Delta G^\circ_{37(\text{bulge})}$, versus free energy of the second least stable duplex stem. (Note that stem free energy was calculated without the inclusion of the free energy of duplex initiation.) Group II bulge loops (black box) and group I bulge loops (gray circle) (Blose et al. 2007). Lines are the least-squares fit of the data points.

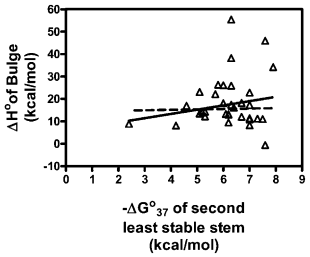

FIGURE 4. Plot of enthalpy change for group II bulge loop formation, ΔH°_{bulge}, versus free energy of the second least stable duplex stem. (Note that stem free energy was calculated without the inclusion of the free energy of duplex initiation.) (Solid line) The least-squares fit of the group II data; (dashed line) the least-squares fit of the group II data for the group I data (Blose et al. 2007).

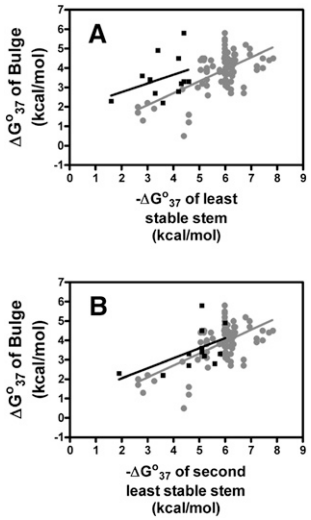

FIGURE 5. (*A*) Plot of free energy change for group II bulge loop formation with three consecutive identical nucleotides, $\Delta G^\circ_{37(bulge)}$, versus free energy of the least stable duplex stem. (*B*) Plot of free energy change for bulge loop formation, $\Delta G^\circ_{37(bulge)}$, versus free energy of the second least stable duplex stem. (Note that stem free energy was calculated without the inclusion of the free energy of duplex initiation.) Group II bulge loops (black box) and group I bulge loops (gray circle) (Blose et al. 2007). Lines are the least-squares fit of the data points.

3.9, 4.0, 1.8, and 1.7 kcal/mol. The two bulge loops that have the largest difference between the measured and predicted values are the sequences CAAC/GU G and GCCU/CG A, 2.3 and 2.6 kcal/mol more destabilizing than predicted. (These are the only two sequences where the predicted and measured values differ by >2 kcal/mol.) It is not obvious why these two bulge loops would not be predicted as well as the other group II bulge loops.

Structural determination of the bulged nucleotide using in-line probing

In-line probing takes advantage of the natural instability of RNA to distinguish between single-stranded and double-stranded regions of RNA (Soukup and Breaker 1999). Single-stranded regions have structural flexibility relative to the A-form geometry of double-helical RNA. This additional flexibility allows single-stranded RNA to sample geometries that align the 2′-O with the phosphate and 5′-O of the phosphodiester bond favoring the transition state for the cleavage of the phosphodiester bond. We first examined the cleavage of a group I bulge loop to determine whether cleavage would occur to the 5′ or 3′ side of a bulged nucleotide. In-line cleavage of the group I bulge loop generated, as expected, a fluorescent tetramer product indicative of cleavage to the 3′ side of the bulged nucleotide (Fig. 1). We then carried out in-line probing of the group II bulge loop shown in Figure 1. The results of this cleavage show that the major fluorescent product (90%) was a tetramer, indicating that the bulged nucleotide was the 3′ adenosine residue, farther from the hairpin loop.

For the four group II hairpins that we analyzed by in-line probing, each produced as the major cleavage product, the fragment that corresponds to the bulged nucleotide was the one farther from the hairpin loop. Because of the positional ambiguity of the bulge and the hairpin loop, it is not obvious how to determine the thermodynamic stability of the stems adjacent to the bulged nucleotide. For example, for the stem between the bulge and the hairpin loop, should the stability of the stem be considered as just the base-paired nucleotides, or include the stabilization due to the terminal mismatch, or also include the destabilization due to the hairpin loop? Table 6 lists the possible stems and thermodynamic stabilities for the first hairpin listed in Table 5. Therefore, it is not possible to relate the position of the bulged nucleotide to the thermodynamics of the adjacent stems as it is not clear how to determine stem stability.

For the first three hairpins in Table 5, the bulged adenosine residue was the one that would have disrupted the less stable nearest-neighbor base pair. For the first two, the red adenosine disrupts a 5′-AU/UA ($\Delta G^\circ_{37} = -1.1$ kcal/mol); while the blue adenosine would have disrupted a 5′-UG/AC base pair ($\Delta G^\circ_{37} = -2.11$ kcal/mol). For the third, the blue

TABLE 6. Thermodynamics of potential stem sequences for 5′ CA U GU$^{G}_{A}$ / FGUAACA^{A}

Bulged nucleotide	Potential end stem	ΔG°_{37} kcal/mol	Potential hairpin stem	ΔG°_{37} kcal/mol	Potential hairpin stem	ΔG°_{37} kcal/mol	Potential hairpin stem	ΔG°_{37} kcal/mol
			Stem only		Stem and first mismatch		Stem and hairpin loop	
5' (Blue) Adenosine	CAU FGUA	-3.2	GU CA	-2.2	GUG CAA	-3.3	GU$^{G}_{A}$ CA^{A}	+0.8
3' (Red) Adenosine	CA FGU	-2.1	UGU ACA	-4.3	UGUG ACAA	-5.4	UGU$^{G}_{A}$ ACA^{A}	-1.3

adenosine residue disrupts a 5′-UA/AU ($\Delta G°_{37} = -1.33$ kcal/mol); while the red adenosine would have disrupted a 5′-AG/UC base pair ($\Delta G°_{37} = -2.08$ kcal/mol). The last hairpin in Table 5 was included to determine if the stability of the nearest-neighbor base pairs was responsible for the positioning of the bulged nucleotide. In this case, the blue adenosine would disrupt a 5′-CA/GU base pair ($\Delta G°_{37} = -2.11$ kcal/mol) that has a nearest-neighbor free energy equal to the free energy of the 5′-AG/UC base pair ($\Delta G°_{37} = -2.08$ kcal/mol) disrupted by the red adenosine (Xia et al. 1998). The bulged nucleotide in the last hairpin in Table 5 is again the one farther from the hairpin despite the fact that each adenosine residue would disrupt a nearest neighbor of equal stability. The melting studies and in-line probing experiments are done under different solvent conditions; the magnesium ion or higher pH of the in-line probing buffer may influence the structure of the group II bulges; therefore, correlations between the in-line structural studies and thermodynamics should be considered with caution.

The structure of a group II RNA containing duplex has been determined by NMR (Popenda et al. 2008). It was found that the bulged nucleotide (the possible bulged nucleotides were two adenosine residues) was the adenosine that led to the least stable stem. The authors also observed a greater conformational flexibility at the bulge site as expected from the introduction of a defect in the duplex. These results and our in-line probing results should caution against using our thermodynamic model of group II bulge loops to suggest structural implications. Additional study of the structure of group II bulge loops in different contexts will be necessary to explain the structural ambiguity of the group II bulge loops.

SUPPLEMENTAL MATERIAL

Supplemental material can be found at http://www.rnajournal.org.

ACKNOWLEDGMENTS

This work was supported by National Science Foundation Grant No. MCB-0744631 and The Paul E. and Mildred L. Hill Fund of Allegheny College.

Received June 7, 2010; accepted October 23, 2010.

REFERENCES

Allawi HT, SantaLucia J Jr. 1997. Thermodynamics and NMR of internal G·T mismatches in DNA. *Biochemistry* **36:** 10581–10594.

Åström H, Williams NH, Strömberg R. 2003. Oligonucleotide based artificial nuclease (OBAN) systems. Bulge size dependence and positioning of catalytic group in cleavage of RNA-bulges. *Org Biomol Chem* **1:** 1461–1465.

Blose JM, Manni ML, Klapec KA, Stranger-Jones Y, Zyra AC, Sim V, Griffith CA, Long JD, Serra MJ. 2007. Non-nearest-neighbor dependence of the stability for RNA bulge loops based on the complete set of group I single-nucleotide bulge loops. *Biochemistry* **46:** 15123–15135.

Borer PN. 1975. In *Handbook of biochemistry and molecular biology: Nucleic acids* (ed. GD Fasman), p. 589. CRC Press, Cleveland, OH.

Borer P, Dengler B, Tinoco I Jr. 1974. Stability of ribonucleic acid double-stranded helices. *J Mol Biol* **86:** 843–853.

Brion P, Westhof E. 1997. Hierarchy and dynamics of RNA folding. *Annu Rev Biophys Biomol Struct* **26:** 113–137.

Cannone JJ, Subramanian S, Schnare MN, Collett JR, D'Souza LM, Du Y, Feng B, Lin N, Madabusi LV, Muller KM, et al. 2002. The comparative RNA web (CRW) site: an online database of comparative sequence and structure information for ribosomal, intron, and other RNAs. *BMC Bioinformatics* **3:** 2. doi: 10.1186/1471-2105-3-2.

Chung KH, Hart CC, Al-Bassam S, Avery A, Taylor J, Patel PD, Vojtek AB, Turner DL. 2006. Polycistronic RNA polymerase II expression vectors for RNA interference based on BIC/miR-155. *Nucleic Acids Res* **34:** e53. doi: 10.1093/nar/gkl143.

Conceicao A, Minetti SA, Remeta DP, Dickstein R, Breslauer KJ. 2010. Energetic signatures of single base bulges: thermodynamic consequences and biological implications. *Nucleic Acids Res* **38:** 97–116.

Doudna JA, Cormack BP, Szostak JW. 1989. RNA structure, not sequence, determines the 5′ splice-site specificity of a group I intron. *Proc Natl Acad Sci* **86:** 7402–7407.

Freier SM, Kierzek R, Jaeger JA, Sugimoto N, Caruthers MH, Neilson T, Turner DH. 1986. Improved free-energy parameters for predictions of RNA duplex stability. *Proc Natl Acad Sci* **83:** 9373–9377.

Harper JW, Logsdon NJ. 1991. Refolded HIV-1 tat protein protects both bulge and loop nucleotides in TAR RNA from ribonucleolytic cleavage. *Biochemistry* **30:** 8060–8066.

Hofacker IL, Fontana W, Stadler PF, Bonhoeffer LS, Tacker M, Schuster P. 1994. Fast folding and comparison of RNA secondary structures. *Monatsh Chem* **125:** 167–168.

Krasovska MV, Sefcikova J, Réblova K, Schneider B, Walter NG, Šponer J. 2006. Cations and hydration in catalytic RNA: Molecular dynamics of the hepatitis delta virus ribozyme. *Biophys J* **91:** 626–638.

Lilley DM. 1995. Kinking of DNA and RNA by base bulges. *Proc Natl Acad Sci* **92:** 7140–7152.

Longfellow CE, Kierzek R, Turner DH. 1990. Thermodynamic and spectroscopic study of bulge loops in oligoribonucleotides. *Biochemistry* **29:** 278–285.

Lu ZJ, Turner DH, Mathews DH. 2006. A set of nearest neighbor parameters for predicting the enthalpy change of RNA secondary structure formation. *Nucleic Acids Res* **34:** 4912–4924.

Mathews DH, Disney MD, Childs JL, Schroeder SJ, Zuker M, Turner DH. 2004. Incorporating chemical modification constraints into a dynamic programming algorithm for prediction of RNA secondary structure. *Proc Natl Acad Sci* **101:** 7287–7292.

Matzke MA, Birchler JA. 2005. RNAi-mediated pathways in the nucleus. *Nat Rev Genet* **6:** 24–35.

McDowell JA, Turner DH. 1996. Investigation of the structural basis for thermodynamic stabilities of tandem GU mismatches: Solution structure of $(rGAG\underline{GU}CUC)_2$ by two-dimensional NMR and simulated annealing. *Biochemistry* **35:** 14077–14089.

Popenda L, Adamiak RW, Gdaniec Z. 2008. Bulged adenosine influence on the RNA duplex conformation in solution. *Biochemistry* **47:** 5059–5067.

Regulski EE, Breaker RR. 2008. In-line probing analysis of riboswitches. *Methods Mol Biol* **419:** 53–67.

Richards EG. 1975. In *Handbook of biochemistry and molecular biology: Nucleic acids* (ed. GD Fasman), p. 197. CRC Press, Cleveland, OH.

Rieger A, Nassal M. 1995. Distinct requirements for primary sequence in the 5′- and 3′-part of a bulge in the hepatitis B virus RNA encapsidation signal revealed by a combined in vivo selection/in vitro amplification system. *Nucleic Acids Res* **23:** 3909–3915.

Roy S, Delling U, Chen CH, Rosen CA, Sonenberg N. 1990. A bulge structure in HIV-1 TAR RNA is required for tat binding and tat-mediated *trans*-activation. *Genes Dev* **4:** 1365–1373.

Schmelzer C, Schweyen RJ. 1986. Self-splicing of group II introns in vitro: Mapping of the branch point and mutational inhibition of lariat formation. *Cell* **46:** 557–565.

Schmidt U, Podar M, Stahl U, Perlman PS. 1996. Mutations of the two-nucleotide bulge of D5 of a group II intron block splicing in vitro and in vivo: Phenotypes and suppressor mutations. *RNA* **2:** 1161–1172.

Serra MJ, Axenson TJ, Turner DH. 1994. A model for the stabilities of RNA hairpins based on a study of the sequence dependence of stability for hairpins of six nucleotides. *Biochemistry* **33:** 14289–14296.

Soukup GA, Breaker RR. 1999. Relationship between internucleotide linkage geometry and the stability of RNA. *RNA* **5:** 1308–1325.

Suzuki H, Zuo Y, Wang J, Zhang MQ, Malhotra A, Mayeda A. 2006. Characterization of RNase R-digested cellular RNA source that consists of lariat and circular RNAs from pre-mRNA splicing. *Nucleic Acids Res* **34:** e63. doi: 10.1093/nar/gkl151.

Tanaka F, Kameda A, Yamamoto M, Ohuchi A. 2004. Thermodynamic parameters based on a nearest-neighbor model for DNA sequences with a single-bulge loop. *Biochemistry* **43:** 7143–7150.

Tinoco I Jr, Bustamante C. 1999. How RNA folds. *J Mol Biol* **293:** 271–281.

Tinsley RA, Furchak JRW, Walter NG. 2007. *Trans*-acting *glmS* catalytic riboswitch: Locked and loaded. *RNA* **13:** 468–477.

Usman N, Ogilvie KK, Jiang MV, Cedergren R. 1987. The automated chemical synthesis of long oligoribonucleotides using 2′-*O*-silylated ribonucleoside 3′-*O*-phosphoramidites on a controlled-pore glass support: synthesis of a 43-nucleotide sequence similar to the 3′-half molecule of an Escherichia coli formylmethionine tRNA. *J Am Chem Soc* **109:** 7845–7854.

Wincott F, DiRenzo A, Shaffer C, Grimm S, Tracz D, Workman C, Sweedler D, Gonzalez C, Scaringe S, Usman N. 1995. Synthesis, deprotection, analysis and purification of RNA and ribozymes. *Nucleic Acids Res* **23:** 2677–2684.

Xia T, SantaLucia J Jr, Burkard ME, Kierzek R, Schroeder SJ, Jiao X, Cox C, Turner DH. 1998. Thermodynamic parameters for an expanded nearest-neighbor model for formation of RNA duplexes with Watson-Crick base pairs. *Biochemistry* **37:** 14719–14735.

Zhu J, Wartell RM. 1999. The effect of base sequence on the stability of RNA and DNA single base bulges. *Biochemistry* **38:** 15986–15993.

Znosko BM, Silvestri SB, Volkman H, Boswell B, Serra MJ. 2002. Thermodynamic parameters for an expanded nearest-neighbor model for the formation of RNA duplexes with single nucleotide bulges. *Biochemistry* **41:** 10406–10417.

Zuker M. 2003. Mfold web server for nucleic acid folding and hybridization prediction. *Nucleic Acids Res* **31:** 3406–3415.